Direct wind measurements of Saharan dust events from Terra and Aqua satellites

Ilan Koren
NASA Goddard Space Flight Center, Greenbelt, Maryland, USA
National Research Council, Washington, DC, USA

Yoram J. Kaufman
NASA Goddard Space Flight Center, Greenbelt, Maryland, USA

Received 19 December 2003; revised 2 February 2004; accepted 20 February 2004; published 25 March 2004.

[1] Wind speed and direction, during Saharan dust episodes are calculated by estimating the movement of the dust plume between the morning observations from Terra and the afternoon observations from Aqua by the MODerate resolution Imaging Spectroradiometer (MODIS). The difference in the position of the dust front (easily identified both near the dust sources and over the ocean) between the Terra and Aqua observations is used to derive the actual wind field of the dust layer. The analysis is used to estimate the near-surface wind properties needed for dust mobilization in the Bodele depression. Comparison with NCEP reanalysis winds shows that NCEP underestimated by factor 2 the actual speed of the dust front progression near the sources and produced an azimuthal spread, three times wider than the measured one. Over the seashore, with more numerous meteorological observations, the NCEP wind field did match very well the dust measurements. *INDEX TERMS:* 0305 Atmospheric Composition and Structure: Aerosols and particles (0345, 4801); 3307 Meteorology and Atmospheric Dynamics: Boundary layer processes; 3322 Meteorology and Atmospheric Dynamics: Land/atmosphere interactions; 3337 Meteorology and Atmospheric Dynamics: Numerical modeling and data assimilation; 3360 Meteorology and Atmospheric Dynamics: Remote sensing. **Citation:** Koren, I., and Y. J. Kaufman (2004), Direct wind measurements of Saharan dust events from Terra and Aqua satellites, *Geophys. Res. Lett.*, *31*, L06122, doi:10.1029/2003GL019338.

1. Introduction

[2] Desert dust changes the radiative energy of the climate system by reflecting and absorbing solar radiation, and indirectly, by changing clouds properties. As a consequence dust affects the hydrological cycle and the dynamic properties of the atmosphere [*Carlson and Prospero*, 1972; *Ginoux and Torres*, 2003]. Global scale models, evaluated by satellite and ground based observations, have been used to simulate dust emission, transport and deposition [*Chin et al.*, 2002].

[3] Surface winds control dust emissions. Models of dust mobilization define differently the dependence of dust emission on the wind speed, however, all of them use a minimal threshold of wind speed above which dust is mobilized [*Ginoux et al.*, 2001, and the references therein].

[4] Saharan dust is emitted to the atmosphere in pulses [*Kubilay et al.*, 2000]. Often the dust events result from collection of many small-scale dust plumes emerging from separated point sources within an area of a few square kilometers [*Koren et al.*, 2003]. *Prospero et al.* [2002] describe the evolution of dust storms and show that dust is emitted from the Sahara from a few, well defined, sources. These sources emit dust when the local environmental properties are suitable (i.e., surface humidity, composition of particles and winds).

[5] One of the most vigorous sources for dust in the Sahara is the Bodele depression (17°N, 18°E) located northeast of Lake Chad, and composed of a series of ephemeral lakes collecting erosion from a few sources [*Mounkaila et al.*, 2003]. The direct sources of alluvium material are the Tibesty Mountains north, and the Ennedi Mountains east of the Bodele. These mountains form a large Caldera-like shape, with its northeast boundary being Egypt's west border. The opening in the Caldera channels the surface winds directly towards the Bodele. Evidence of such wind channeling is observed from satellite images by visually following the wind channels on the surface, from south of the Nile delta in Egypt, through the Tibesty-Ennedi passage and then over the Bodele toward the Sahel in the southwest.

[6] The propagation of dust storms over the Atlantic Ocean was observed already by *Carlson and Prospero* [1972] using Advanced Very High Resolution Radiometer (AVHRR) images. They detected the locations of the dust fronts (leading edge) by combining surface measurements (ship), radiosondes, in situ aircraft measurements and satellite images.

[7] In this study we analyze all the dust storms observed during January–April 2003 over the Bodele and calculate the wind speed and direction of the dust movement for each event. The dust progression is derived from the average displacement of the dust front between the morning-pass of Terra and the three hours later afternoon-pass of Aqua. MODIS daily observations with the visible channels [*Salomonson et al.*, 1989] are used in the analysis. Terra in a descending orbit passes over the Sahara in approximately at 10:30 am GMT and Aqua in an ascending orbit passes over the same area approximately at 1:30 pm GMT. Note that the wind field may change between the Terra and Aqua observations. *Ginoux*

0094-8276/04/2003GL019338$05.00

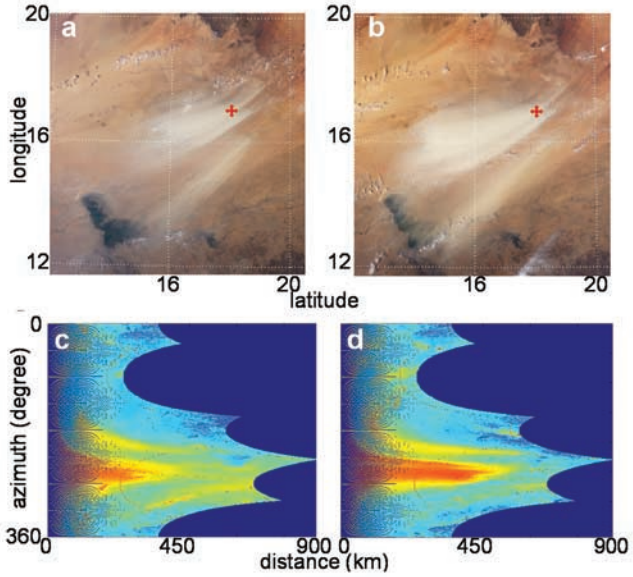

Figure 1. Upper images: MODIS true color images of dust emitted from the Bodele depression on March 12, 2003. On the left side (a) the Terra image at 9:15 GMT and on the right side (b) the same event in Aqua at 12:15 GMT. The center of the Bodele depression (17°N, 18°E) marked in red. Lower images: Polar transformation of the blue channel of the upper images. On the left side (c) the polar transformation of Terra and on the right side (d) the transformation of the plume 3 hours later from Aqua. The red points are the reference (origin) for the transformation. The dark blue color represents empty pixels. The border between the dark blue to the other colors is the polar mapping of the borders of the images.

and Torres [2003] analyzed the diurnal cycle of the wind pattern showing higher likelihood of stronger winds in the morning than in the afternoon. Therefore the measured wind vector in this study represents the average wind around noontime in the geographic region described by the location and displacement of the dust front.

2. Analysis

[8] Dust events mobilized by strong winds are characterized by high reflectance of the suspended matter, above the packed background. Both over land and ocean the plumes have a narrow and focused shape, bounded within the line of maximum gradient in optical depth. Dust events near the source exhibit a sharp gradient in optical depth along the front line of the plume followed by high optical depth with small variations (see Figures 1a and 1b).

[9] We define the front point (see Figure 2) as the location where the optical depth is half of the average value in the bulk part of the plume. Over the ocean the gradient is already not as sharp. The line that connects the front points in the leading edge of the plume defines the front line. The displacement of the dust front between the Terra and Aqua observations is defined as the average difference in the location of the front line, along the direction of propagation. Such definition of the front line allows calculation of the displacement of the dust event between Terra and Aqua, independently of the magnitude of the dust optical depth.

[10] To take advantage of the MODIS 0.5 km resolution data for precise determination of the front location and for cloud screening, we use the MODIS measured spectral reflectance, rather than the optical thickness that is archived at 10 km resolution. Over the ocean the differences between the red (645 nm) and the blue (470 nm) reflectance is used, in order to enhance the contrast between the dust and the ocean. Over the land we use the blue reflectance only. Note that gradients in the reflectances are proportional to the gradient in the dust optical thickness.

[11] Figure 1 shows the Terra (Figure 1a) and Aqua (Figure 1b) MODIS true color images of dust emitted from the Bodele depression (17°N, 18°E, marked in the images) on March 12, 2003. Figure 2 shows a contour plot of the line of maximum gradient in the blue reflectance of the same images. Note that the contours of the two plume structures are very similar one to another.

[12] To calculate the average displacement and direction (azimuth) of the dust front we transformed the satellite images from a Cartesian coordinate set to a polar set where the origin is located at the center of the dust source over land or in the beginning of the plume over the ocean. The lower images in Figure 1 (Figures 1c and 1d) are the transformed images in the blue channel of Figures 1a and 1b, respectively. The y axis is the azimuth in degrees and the x axis is the distance from the origin (marked as red dot in Figures 1a and 1b), directly proportional to the wind speed in the dust layer. Furthermore, we can measure the uncertainty in the azimuth of the wind vector as the width of the dust plume along the y scale and the uncertainty in front location as the width of the front (x scale).

[13] Figure 3 shows plots of the average cross sections of the dust fronts, Terra in blue and Aqua in red. The cross section is calculated by summing the rows of the dust plume in the polar image and normalizing the result (sum of the reflectances) to one. We estimate the uncertainty in the front

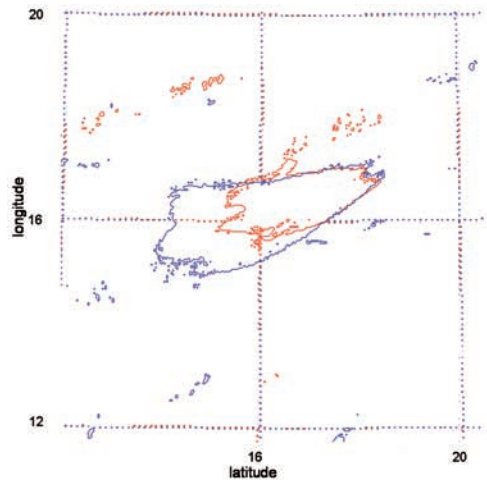

Figure 2. Contour plot of the line of maximum gradient in the blue reflectance. The red line is of the dust plume in the Terra image and the blue line is of Aqua. The propagation of the plume can be estimated by the average distance of the front lines.

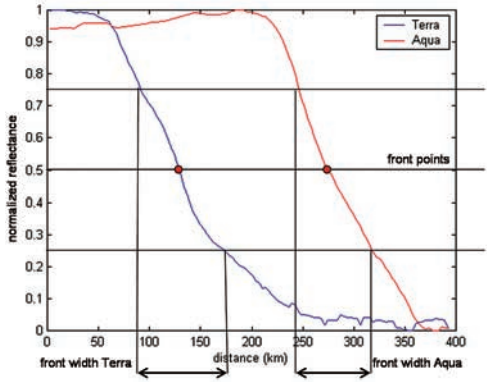

Figure 3. Fronts cross sections of the March 12, 2003 dust event in the Bodele depression. The uncertainty in the front displacement is estimated by the horizontal distance of the 25% reflectance to 75%.

displacement as the difference between the widths of the fronts defined by the location of the points that correspond to 25% and 75% of the maximum reflectance in relation to the 50% point.

3. Analysis of the Wind Field

[14] We analyzed 15 dust events, all but two events emitted from the Bodele Depression during the winter and spring of 2003. The omitted two events were not covered by Terra or Aqua. The average wind speed is 13 m/s with standard deviation of 1 m/s, in accord with average uncertainty per single measurement of 1.2 m/s. The average direction is 248° ± 8°.

[15] The results were compared to NCEP 12:00 GMT, 2.5° × 2.5° lat. × long resolution reanalysis winds for the grid point of the Bodele depression at 5 height levels (1000, 925, 850, 700, 600 mb) [*Kalnay et al.*, 1996]. Such reanalysis databases are the input for dust models for activation of sources and dust transport. The near surface winds (925 mb) were consistently closer in azimuth and in speed to the measured winds though significantly weaker. The mean 925 mb wind speed is 7.2 ± 2.5 m/s, 50% weaker than measured, and the average azimuth is 238° ± 24°, close to the measured azimuth of 248° but with a large standard deviation. In Figure 4, the measured winds (blue) and the reanalysis winds in three pressure levels (1000, 925, 850) are plotted in polar coordinates.

[16] We also analyzed dust wind speed over locations with more numerous radiosonde data that act as control points in the reanalysis model, expecting a better fit. Results are given for two cases near Dakar, one case over the Atlantic Ocean halfway towards Brazil and one case offshore of the south Mediterranean shore in Libya (February 5, 2003). The results are displayed in Figure 5. Over Dakar (March 02, 2003) a dust plume is observed crossing the coastline from a nearby source. A perfect match is obtained between the measured wind (blue star) and the model wind for the 925 mb level (blue circles). On the following day, another dust event was measured north of Dakar, in this case (marked red in Figure 5) the direction matches perfectly (azimuth 274) for the surface wind

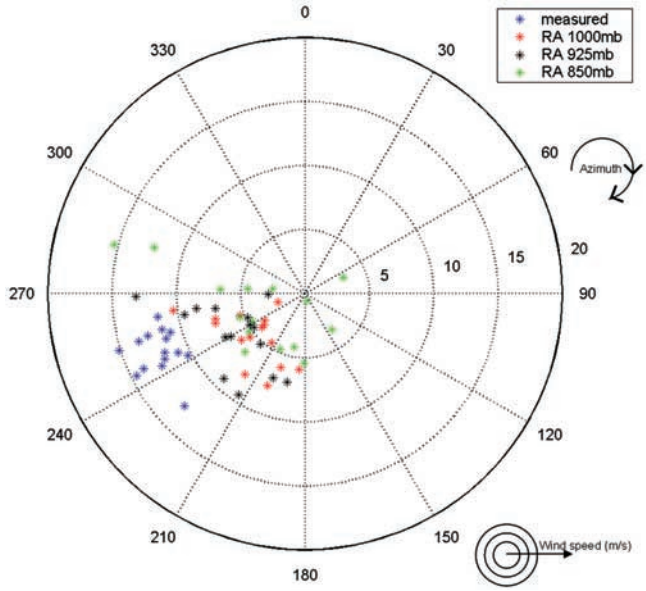

Figure 4. Direct wind measurements over the Bodele depression (blue), and the model reanalysis results at the surface (red), 925 mb (black), and 850 mb (green). The dashed circles are wind speed lines of 0m/s in the origin 5, 10, 15 and 20 m/s and the numbers on the outer circle are the wind direction in degrees from the north (see illustrations).

(1000 mb) but the model wind is 23% stronger. The third case (in black), was for a mature plume halfway across the ocean, April 30, 2003, 1000 km of the west cost of Africa. The best match between the measured wind and the model was for height of 700 mb, with a perfect azimuth match

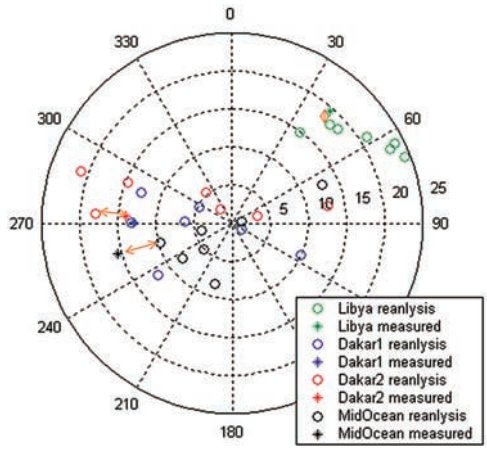

Figure 5. Direct wind measurements in locations where the reanalysis model is expected to have a better agreement with measurements. The stars represent the wind measurements derived from the displacement of the dust fronts and the circles represent the model winds direction and speed in 7 pressure levels 1000 mb to 400 mb. The best agreement is defined by both direction and speed (the orange arrow links the best fit to the measurement).

but a 30% weaker wind. The 700 mb height of the dust is in agreement with Lidar measurements and models [*Karyampudi et al.*, 1999]. The last case, over the Mediterranean, we found almost perfect matches (5% difference) in both speed and direction between the 950 mb winds and the measurement.

4. Summary and Discussion

[17] MODIS data collected from the Terra and Aqua satellites are used to calculate near surface winds close to the dust sources and along the transport lines. Knowledge of the wind field is important to understand the process of dust generation.

[18] The measured winds over the Bodele depression are consistent in direction (238° ± 8° azimuth) probably due to wind channeling in the Tibesti region. Furthermore, the consistency of the measured dust speed in the Bodele of 13 ± 1 m/s is in agreement with the presence of a threshold in the surface wind speed needed for dust production. The minimum measured wind value of 10–11 m/s can be a measure to the threshold velocity for dust emission from the Bodele.

[19] The wind is derived from the displacement in the dust fronts, therefore, it measures the average wind speed and direction, in the dust layer, for the period between the overpass of Terra and Aqua. Since the dust fronts are 150–300 km from the center of the Bodele, it can be expected that the dust is close to the surface and the measured winds are most likely near surface winds [*Chiapello et al.*, 1995].

[20] Near the sources in the Sahara, NCEP wind reanalysis underestimates the actual dust wind speed by factor of 2. Much better fit, within 8–30%, was found near the African seashore, a region better populated with meteorological observatories. The reanalysis winds at the source are used as input for models of dust activation and transport. It is possible that the complex dependence of the dust activation models on the surface winds results from an attempt to correct some of these systematic biases in the reanalysis wind field.

[21] **Acknowledgments.** This research was performed while I.K. held a National Research Council Research Associateship Award at NASA/GSFC.

References

Carlson, T. N., and J. M. Prospero (1972), The large scale movement of Saharan air outbreaks over the northern equatorial Atlantic, *J. Appl. Meteorol.*, *11*, 283–297.

Chiapello, I., et al. (1995), An additional low layer transport of Sahelian and Saharan dust over the north-eastern tropical Atlantic, *Geophys. Res. Lett.*, *22*, 3191–3194.

Chin, M., P. Ginoux, S. Kinne, O. Terres, B. N. Holben, B. N. Duncan, R. V. Martin, J. A. Logan, A. Higurashi, and T. Nakajima (2002), Tropospheric aerosol optical thickness from the GOCART model and comparisons with satellite and Sun photometer measurements, *J. Atmos. Sci.*, *59*, 461–483.

Ginoux, P., and O. Torres (2003), Empirical TOMS index for dust aerosol: Applications to model validation and source characterization, *J. Geophys. Res.*, *108*(D17), 4534, doi:10.1029/2003JD003470.

Ginoux, P., M. Chin, I. Tegen, J. Prospero, B. Holben, O. Dubovik, and S.-L. Lin (2001), Sources and distributions of dust aerosols simulated with the GOCART model, *J. Geophys. Res.*, *106*, 20,555–20,273.

Kalnay, E., et al. (1996), The NCEP/NCAR 40-year reanalysis project, *Bull. Am. Meteorol. Soc.*, *77*, 431–437.

Karyampudi, V. M., et al. (1999), Validation of the Saharan dust plume conceptual model using lidar, Meteosat and ECMWF data, *Bull. Am. Meteorol Soc.*, *80*, 1045–1075.

Koren, I., J. H. Joachim, H. Joseph, and P. Israelevich (2003), Detection of dust plumes and their sources in northeastern Libya, *Can. J. Remote Sens.*, *29*, 792–796.

Kubilay, N., S. Nickovic, C. Moulin, and F. Dulac (2000), An illustration of the transport and deposition of mineral dust onto the eastern Mediterranean, *Atmos. Environ.*, *34*, 1293–1303.

Mounkaila, M., L. Herrmann, T. Gaiser, and T. Maurer (2003), Spectral and mineralogical properties of potential dust sources on a transect from Sahara to Sahel in Chad, paper presented at 2nd Workshop on Mineral Dust, Paris, Lab. Interuniv. des Syst. Atmos., Paris, 10–12 September.

Prospero, J. M., P. Ginoux, O. Torres, S. E. Nicholson, and T. E. Gill (2002), Environmental characterization of global sources of atmospheric soil dust identified with the Nimbus 7 Total Ozone Mapping Spectrometer (TOMS) absorbing aerosol product, *Rev. Geophys.*, *40*(1), 1002, doi:10.1029/2000RG000095.

Salomonson, V. V., W. L. Barnes, P. W. Maymon, H. E. Montgomery, and H. Ostrow (1989), MODIS: Advanced facility instrument for studies of the Earth as a system, *IEEE Trans. Geosci. Remote Sens.*, *27*, 145–153.

Y. J. Kaufman and I. Koren, NASA Goddard Space Flight Center, Greenbelt, MD 20771, USA. (ilank@climate.gsfc.nasa.gov)